

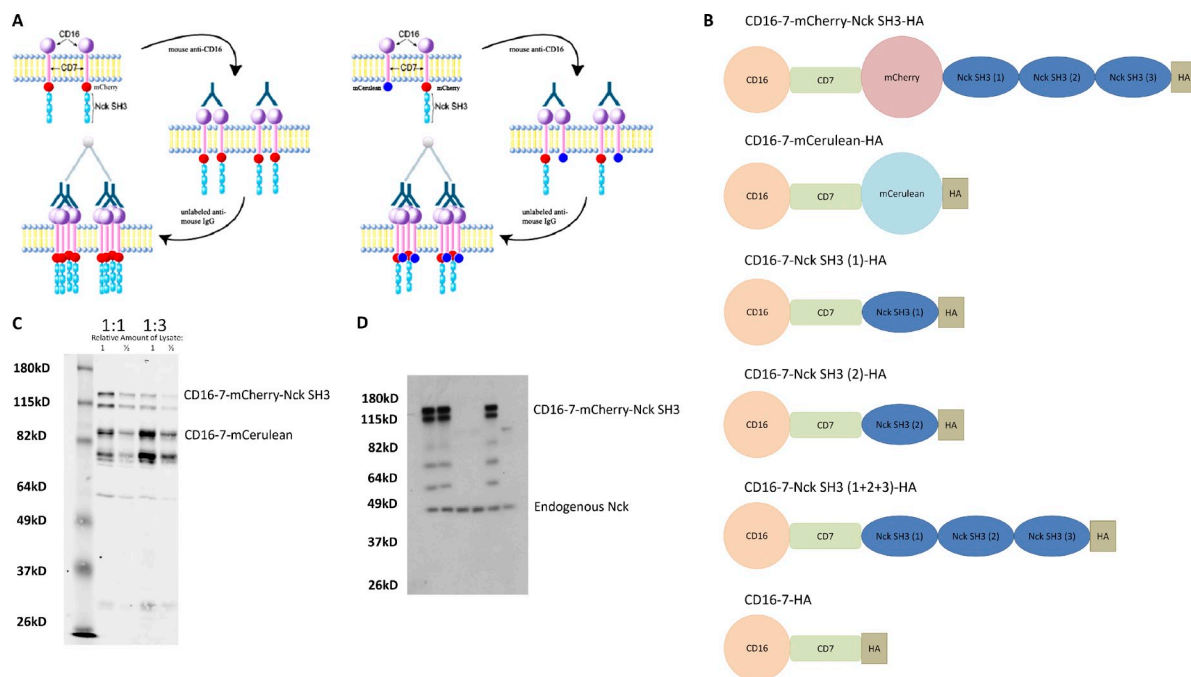
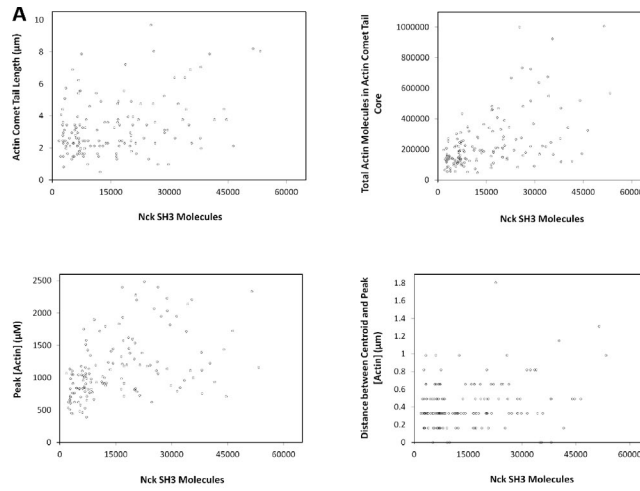
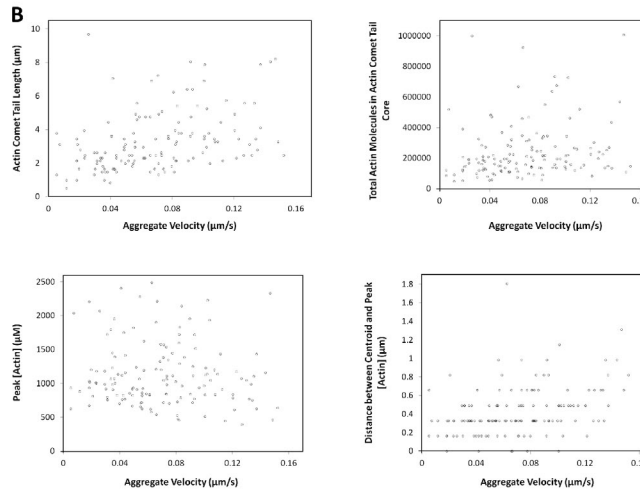
Ditlev et al., <http://www.jcb.org/cgi/content/full/jcb.201111113/DC1>

Figure S1. **Antibody-induced aggregation methodology, fusion protein design, and fusion protein expression in transfected cells.** (A) A schematic of antibody aggregation used in both 100% Nck SH3 density experiments (left) and variable Nck SH3 density experiments (right). (B) Diagrams of CD16-7 fusion proteins used in Nck density studies and mixed Nck aggregation studies. The top two fluorescently labeled constructs are used in actin comet tail and density studies in Figs. 1–5. The bottom four constructs are used in WIP KO or WT MEF and N-WASp KO or WT MEF studies and mixed Nck SH3 studies in Figs. 6 and S3. (C) Western blot–detected expression of two of the transfectants: 50% Nck SH3 and 50% dummy (1:1) and 25% Nck SH3 and 75% dummy (1:3). A double band is observed for each CD16-7 fusion protein: the top band is the full-length fusion protein, whereas the bottom band is a cleaved fusion protein lacking the CD16 domain. (D) A Western blot demonstrating CD16-7-mCherry-Nck SH3-HA versus endogenous Nck expression in transfected NIH-3T3 cells.



Aggregate Size vs. Actin Comet Tail Characteristics



Aggregate Velocity vs. Actin Comet Tail Characteristics

Figure S2. **Aggregate size and velocity are not well correlated with measured actin comet tail characteristics.** (A) Plots correlating the number of Nck SH3 molecules in aggregates with actin comet tail length (top left), total number of actin molecules in the comet tail core (top right), peak [actin] in the comet tail (bottom left), and distance between aggregate center and peak [actin] (bottom right). (B) Plots correlating the velocity of Nck SH3 aggregates with actin comet tail length (top left), total number of actin molecules in the comet tail core (top right), peak [actin] in the comet tail (bottom left), and distance between aggregate center and peak [actin] (bottom right).

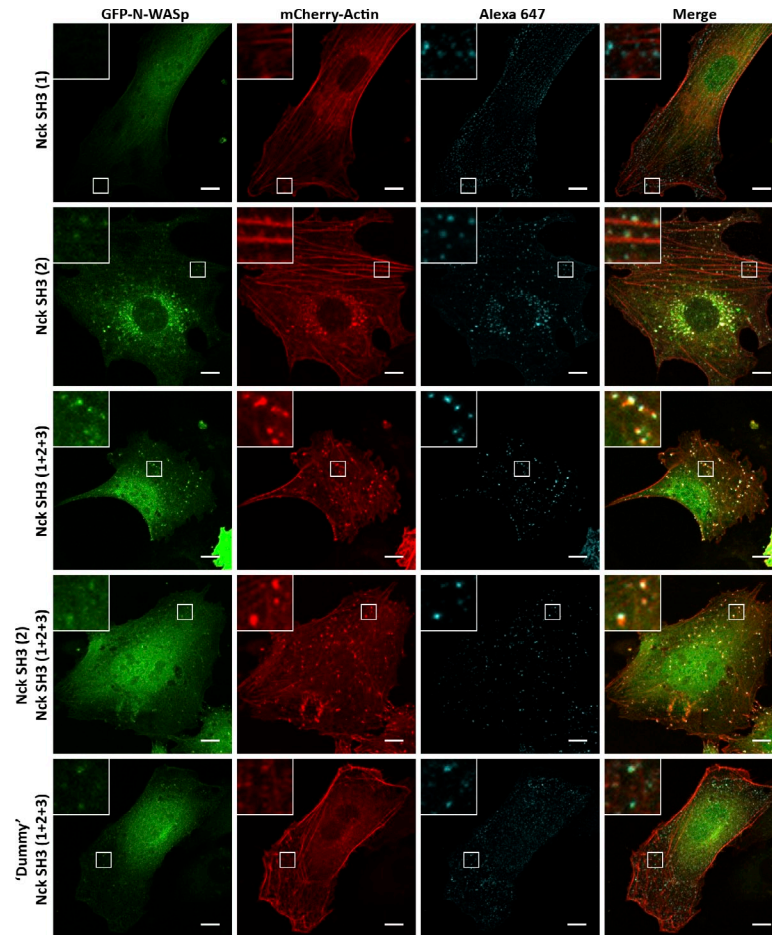


Figure S3. **Full activation of N-WASp requires both Nck SH3 (2) and Nck SH3 (1+2+3) in aggregates.** Confocal microscopy images of NIH-3T3 cells cotransfected with mCherry-actin, GFP-N-WASp, and CD16-7-Nck SH3 (1) or CD16-7-Nck SH3 (2), CD16-7-Nck SH3 (1+2+3), CD16-7-dummy, or a combination of CD16 fusion proteins. For all images, mCherry-actin is red, GFP-N-WASp is green, and CD16 aggregates are cyan. Nck SH3 (1) aggregates (top) did not recruit GFP-N-WASp or induce actin polymerization. Nck SH3 (2) aggregates (second from top) and Nck SH3 (1+2+3)/dummy aggregates (bottom) recruited GFP-N-WASp and induced actin polymerization in the form of actin spots. Both Nck SH3 (1+2+3) (middle) and Nck SH3 (2)/Nck SH3 (1+2+3) (second from bottom) aggregates induce actin comet tail-like structures. Higher magnifications of clusters are shown in the insets. Bars, 10 μ m.

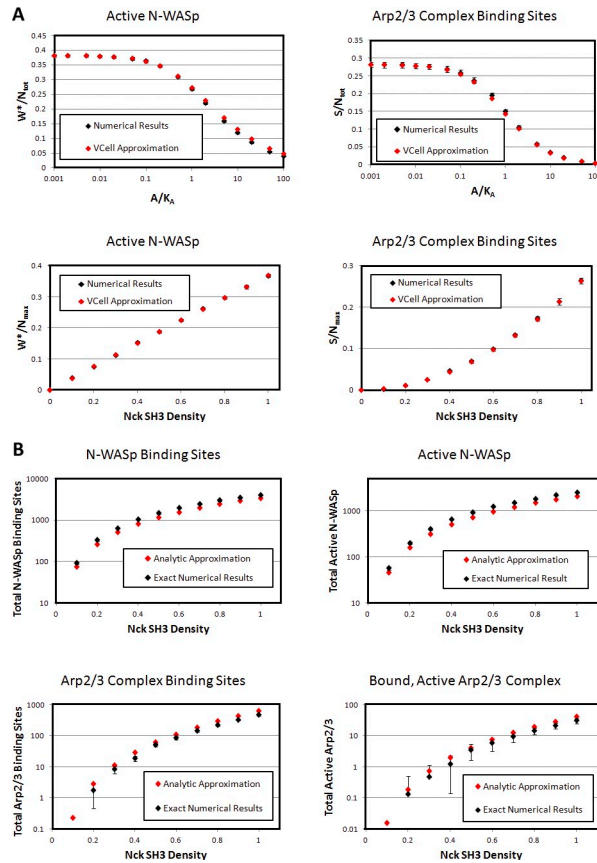
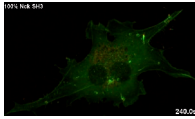
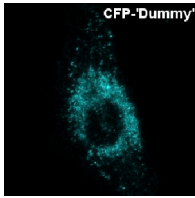


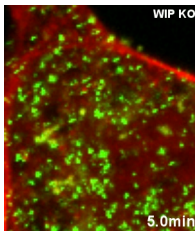
Figure S4. **Exact numerical results and analytical approximations used in the Virtual Cell are sufficiently similar to allow for the approximation to be used in the Virtual Cell model.** (A and B) Graphs displaying the similarity between the Virtual Cell approximations used to describe N-WASp and Arp2/3 complex binding and exact numerical calculations of the number of N-WASp and Arp2/3 complex molecules recruited to the Nck SH3 patch in both the 2:2:1 and 4:2:1 reaction schemes. Error bars are SDs. (A) Comparison of Virtual Cell predictions of N-WASp and Arp2/3 complex binding with exact numerical calculations using the 2:2:1 Nck/N-WASp/Arp2/3 reaction scheme in large 2D lattices. Top plots illustrate the equilibrium-activated N-WASp (left) and Arp2/3 complex binding sites (right) as a function of cytosolic Arp2/3 complex concentration when Nck density is 100% in both Virtual Cell (VCell) approximations and exact numerical calculations. Bottom plots illustrate activated N-WASp (left) and Arp2/3 complex (right) as functions of Nck density for the fixed value of $A/K_A = 0.07$, which is the steady-state ratio of bound and activated Arp2/3 complex to cytosolic Arp2/3 complex in our Virtual Cell simulations. (B) Comparison of Virtual Cell predictions of N-WASp and Arp2/3 complex binding with exact numerical calculations using the 4:2:1 Nck/N-WASp/Arp2/3 reaction scheme in a 30×30 square lattice at varying Nck densities. Top plots illustrate N-WASp binding sites (left) and active N-WASp molecules (right) in Virtual Cell predictions and exact numerical calculations. Bottom plots illustrate Arp2/3 complex binding sites (left) and bound and activated Arp2/3 complex (right) in Virtual Cell predictions and exact numerical calculations. As can be appreciated, although the Virtual Cell approximations overpredict the number of Arp2/3 complex binding sites and active Arp2/3 complexes across the range of Nck densities, the approximations capture the density-dependent variation in the curves and lie within the error bars of the exact numerical predictions, indicating that the Virtual Cell predictions are reliable for predicting actin polymerization downstream of the 4:2:1 Arp2/3 complex activation mechanism.



Video 1. **100% Nck SH3 aggregates induce actin comet tail formation.** NIH-3T3 fibroblasts were transfected with CD16-7-mCherry-Nck SH3-HA (red) and GFP-actin (green). After Nck SH3 domain aggregation, images were analyzed by time-lapse confocal microscopy using a spinning-disc confocal microscope (UltraView). Frames were obtained every 30 s for 5.5 min.



Video 2. **Increasing Nck SH3 density induces a nonlinear increase in actin polymerization.** NIH-3T3 fibroblasts were transfected with CD16-7-mCherry-Nck SH3-HA, YFP-actin, and/or CD16-7-dummy-HA. After Nck SH3 domain and/or dummy aggregation, images were analyzed by time-lapse confocal microscopy using a laser-scanning confocal microscope (LSM 780). Frames were obtained every minute for 12 min.



Video 3. **WIP is necessary for Nck SH3-induced actin polymerization.** WIP WT or KO MEFs were transfected with CD16-7-mCherry-Nck SH3-HA (green) and mCherry-actin (red); KO MEFs were rescued with transfected GFP-WIP (blue). After Nck SH3 domain aggregation, images were analyzed by time-lapse confocal microscopy using a laser-scanning confocal microscope (LSM 780). Frames were obtained every minute for 9 min.

Table S1. **Fluorescence calculations to test for autoquenching of mCherry in aggregates**

| | Total molecules (Western blot) | Fluorescent cells | Total fluorescence | Fluorescence/cell | Molecules/cell | Fluorescence/molecule |
|---|-----------------------------------|-------------------|--------------------|-------------------|----------------|-----------------------|
| Control (no antibody-induced aggregation) | 3.10506×10^{11} | 88 | 13888914 | 157828.57 | 888557 | 0.177623461 |
| Experiment (antibody-induced aggregation) | 3.10506×10^{11} | 35 | 5758937 | 164541.06 | 888557 | 0.185177833 |

Fluorescence/molecule calculations in control and experimental cells are 96% similar (0.178/0.185), indicating that fluorescence autoquenching has little, if any, effect on fluorescence per molecule calculations. Fluorescence autoquenching does not affect fluorescent quantification of CD16-7-mCherry-Nck SH3 aggregates. Fluorescence per molecule calculations in control (no CD16-7-mCherry-Nck SH3 aggregation) and experimental (CD16-7-mCherry-Nck SH3 aggregation) cells reveal that increased mCherry concentration caused by aggregation does not result in autoquenching of mCherry fluorescence.

Table S2. Protein names and descriptions used in the Virtual Cell simplified actin dendritic nucleation model

| Protein name | Model name | Description |
|---------------------------------------|---------------|---|
| G-actin | Gt | ATP form of G-actin |
| | Gd | Sum of ADP-Pi and ADP forms of G-actin |
| F-actin | Fi | Sum of ATP and ADP-Pi forms of F-actin |
| | Fd | ADP form of F-actin |
| Barbed ends | Barb T | ATP barbed end |
| | Barb I | ADP-Pi barbed end |
| | Barb D | ADP barbed end |
| Pointed ends | Point T | ATP pointed end |
| | Point I | ADP-Pi pointed end |
| | Point D | ADP pointed end |
| β -thymosin | Bthy | |
| β -thymosin-bound G-actin | Bthy Gt | ATP form of G-actin bound to β -thymosin |
| | Bthy Gd | Sum of ADP-Pi and ADP forms of G-actin bound to β -thymosin |
| Profilin | Prof | |
| Profilin bound to G-actin | Prof Gt | ATP form of G-actin bound to profilin |
| | Prof Gd | Sum ADP-Pi and ADP forms of G-actin bound to profilin |
| Cofilin | Cof | |
| Cofilin bound to F-actin | Cof Fd | Cofilin bound on an ADP-F-actin subunit |
| | Cof Fd2 | Two cofilins bound on adjacent ADP-F-actin subunits |
| Capping protein | Cap | |
| Capping protein bound to a barbed end | Cap Barb | A lumped variable representing capped barbed ends of the ATP, ADP-Pi, and ADP form |
| Arp2/3 | Arp2/3 | |
| Activated Arp2/3 | Active Arp2/3 | Membrane-bound species consisting of an N-WASp and an Arp2/3 that participates in branching reactions |
| Arp2/3 branch points | Branch I | A single species describing a pointed end in any form, an Arp2/3, and an F-actin subunit in either the ATP or ADP-Pi form |
| | Branch D | A single species describing a pointed end in any form, an Arp2/3, and an F-actin subunit in the ADP form |
| Activated N-WASp | Active N-WASp | Membrane-bound species defined as consisting of an Nck SH3 and an N-WASp that can bind Arp2/3 |
| Nck SH3 domains | Nck SH3 | Membrane-bound species that binds N-WASp |
| N-WASp | N-WASp | Freely diffusing N-WASp in the cytosol, which can bind Nck SH3 domains |
| WIP-bound N-WASp | WIP N-WASp | Freely diffusing WIP-bound N-WASp in the cytosol, which can bind two Nck SH3 domain molecules |

Table S3. Global parameters

| Parameter name | Unit | Functional form/value | Comment |
|-------------------|---------------|---|---|
| ATP | μM | 10,000 | Typical cellular concentration of ATP, assumed buffered |
| ADP | μM | 2,000 | Typical cellular concentration of ADP, assumed buffered |
| Pi | μM | 2,000 | Typical cellular concentration of inorganic phosphate, assumed buffered |
| All F-actin | μM | $F_i + F_d + \text{Cof}F_d + 2.0 \times \text{Coff}F_d + \text{PointT} + \text{PointI} + \text{PointD} + \text{BarbT} + \text{BarbI} + \text{BarbD} + \text{CapBarb} + 2.0 \times (\text{BranchI}_{\text{cyt}} + \text{BranchD}_{\text{cyt}})$ | Sum of all forms of polymerized actin |
| All pointed ends | μM | $\text{PointT} + \text{PointI} + \text{PointD} + \text{BranchI} + \text{BranchD}$ | Sum of free and Arp2/3 capped pointed ends |
| Pointed end total | μM | $\text{PointT} + \text{PointI} + \text{PointD}$ | Sum of free pointed ends |
| Barbed end total | μM | $\text{BarbT} + \text{BarbI} + \text{BarbD}$ | Sum of free barbed ends |
| BrF | 1 | $(\text{BranchI} + \text{BranchD})/\text{AllPointedEnds}$ | The fraction of pointed ends capped by Arp2/3. This is used as a measure of the fraction of F-actin bound in the network (as opposed to detached, freely diffusing filaments) |
| L | 1 | $\text{AllFActin}/\text{AllPointedEnds}$ | The average length of a filament, given in number of subunits |
| Fi stability | 1 | $((F_i/\text{PointedEndTotal}) + (F_i/\text{PointedEndTotal})^3)/(1 + (F_i/\text{PointedEndTotal}) + (F_i/\text{PointedEndTotal})^3)$ | Function that provides stability to certain reactions involving F_i , as described below |
| Fd stability | 1 | $((F_d/\text{PointedEndTotal}) + (F_d/\text{PointedEndTotal})^3)/(1 + (F_d/\text{PointedEndTotal}) + (F_d/\text{PointedEndTotal})^3)$ | Function that provides stability to certain reactions involving F_d , as described below |
| barbK1 | s^{-2} | $\text{koff}_{\text{barbI}} \times \text{koff}_{\text{barbD}} + \text{koff}_{\text{barbI}} \times \text{kbarb}_{\text{ID}} \times \text{Pi} + \text{koff}_{\text{barbD}} \times \text{kbarb}_{\text{DI}}$ | Parameter required when lumping barbed-end reactions with G-actin |
| barbK2 | s^{-2} | $\text{kG}_{\text{DT}} \times r_{\text{hydrolysis}} + \text{kon}_{\text{barbT}} \times \text{BarbedEndTotal} \times r_{\text{hydrolysis}} + \text{kG}_{\text{DT}} \times \text{koff}_{\text{barbT}}$ | Parameter required when lumping barbed-end reactions with G-actin |
| barbprofK1 | s^{-2} | $\text{koff}_{\text{barb}} \times \text{prof}_{\text{eff}} \times \text{Prof}_{\text{cyt}} \times \text{koff}_{\text{barb}} \times \text{prof}_{\text{eff}} \times \text{Prof}_{\text{cyt}} + \text{koff}_{\text{barb}} \times \text{prof}_{\text{eff}} \times \text{Prof}_{\text{cyt}} \times \text{kbarb}_{\text{ID}} \times \text{Pi} + \text{koff}_{\text{barb}} \times \text{prof}_{\text{eff}} \times \text{Prof}_{\text{cyt}} \times \text{kbarb}_{\text{DI}}$ | Parameter required when lumping barbed-end reactions with profilin-G-actin |
| barbprofK2 | s^{-2} | $\text{kG}_{\text{DT}} \times r_{\text{hydrolysis}} + \text{kon}_{\text{barb}} \times \text{prof}_{\text{eff}} \times \text{BarbedEndTotal} \times r_{\text{hydrolysis}} + \text{kG}_{\text{DT}} \times \text{koff}_{\text{barb}} \times \text{prof}_{\text{eff}} \times \text{Prof}_{\text{cyt}}$ | Parameter required when lumping barbed-end reactions with profilin-G-actin |
| barbprofQ DI | s^{-5} | $\text{kG}_{\text{DI}} \times \text{barbprofK1} \times \text{barbprofK2} + \text{koff}_{\text{barb}} \times \text{prof}_{\text{eff}} \times \text{Prof}_{\text{cyt}} \times \text{kbarb}_{\text{DI}} \times \text{kon}_{\text{barb}} \times \text{prof}_{\text{mod}} \times \text{BarbedEndTotal} \times \text{barbprofK2}$ | Parameter required when lumping barbed-end reactions with profilin-G-actin |
| barbprofQ ID | s^{-5} | $\text{kG}_{\text{ID}} \times \text{Pi} \times \text{barbprofK1} \times \text{barbprofK2} + \text{koff}_{\text{barb}} \times \text{prof}_{\text{eff}} \times \text{Prof}_{\text{cyt}} \times \text{kbarb}_{\text{ID}} \times \text{Pi} \times \text{kon}_{\text{barb}} \times \text{prof}_{\text{mod}} \times \text{BarbedEndTotal} \times \text{barbprofK2}$ | Parameter required when lumping barbed-end reactions with profilin-G-actin |
| barbQ DI | s^{-5} | $\text{kG}_{\text{DI}} \times \text{barbK1} \times \text{barbK2} + \text{koff}_{\text{barbD}} \times \text{kbarb}_{\text{DI}} \times \text{kon}_{\text{barbI}} \times \text{BarbedEndTotal} \times \text{barbK2}$ | Parameter required when lumping barbed-end reactions with G-actin |
| barbQ ID | s^{-5} | $\text{kG}_{\text{ID}} \times \text{Pi} \times \text{barbK1} \times \text{barbK2} + \text{koff}_{\text{barbI}} \times \text{kbarb}_{\text{ID}} \times \text{Pi} \times \text{kon}_{\text{barbD}} \times \text{BarbedEndTotal} \times \text{barbK2}$ | Parameter required when lumping barbed-end reactions with G-actin |
| cytI DI | s^{-11} | $((\text{kon}_{\text{bthyD}} \times \text{Bthy}_{\text{cyt}} \times \text{cytQ}_{\text{DI}} \times (((\text{koff}_{\text{profD}} + \text{kprof}_{\text{DI}}) \times \text{cytK1}) + (\text{kprof}_{\text{DT}} \times \text{kon}_{\text{profT}} \times \text{Prof}_{\text{cyt}} \times \text{kG}_{\text{TD}}))) + (\text{kprof}_{\text{DI}} \times ((\text{cytK1} \times \text{kon}_{\text{profI}} \times \text{Prof}_{\text{cyt}} \times \text{cytQ}_{\text{ID}}) + (\text{kprof}_{\text{DT}} \times \text{kon}_{\text{profT}} \times \text{Prof}_{\text{cyt}} \times \text{kG}_{\text{TD}} \times \text{cytQ}_{\text{DI}}))))))$ | Parameter required when lumping cytosolic reactions |
| cytI ID | s^{-11} | $((\text{kon}_{\text{bthyD}} \times \text{Bthy}_{\text{cyt}} \times \text{cytQ}_{\text{ID}} \times (((\text{koff}_{\text{profD}} + \text{kprof}_{\text{ID}} \times \text{Pi})) \times \text{cytK1}) + (\text{kprof}_{\text{TD}} \times \text{kG}_{\text{DT}} \times \text{koff}_{\text{profT}}))) + (\text{kprof}_{\text{ID}} \times \text{Pi} \times \text{cytQ}_{\text{DI}} \times ((\text{cytK1} \times \text{kon}_{\text{profD}} \times \text{Prof}_{\text{cyt}}) + (\text{kprof}_{\text{DT}} \times \text{kon}_{\text{profT}} \times \text{Prof}_{\text{cyt}} \times \text{kG}_{\text{TD}}))))))$ | Parameter required when lumping cytosolic reactions |
| cytK1 | s^{-2} | $((\text{kprof}_{\text{DT}} \times \text{kG}_{\text{DT}}) + (\text{kG}_{\text{DT}} \times \text{koff}_{\text{profT}}) + (\text{kprof}_{\text{DT}} \times \text{kon}_{\text{profT}} \times \text{Prof}_{\text{cyt}}))$ | Parameter required when lumping cytosolic reactions |
| cytK3 | s^{-2} | $((\text{koff}_{\text{profD}} \times \text{koff}_{\text{profD}}) + (\text{koff}_{\text{profD}} \times \text{kprof}_{\text{DI}}) + (\text{koff}_{\text{profD}} \times \text{kprof}_{\text{ID}} \times \text{Pi}))$ | Parameter required when lumping cytosolic reactions |
| cytK4 | s^{-4} | $((\text{cytK1} \times \text{cytK3}) + (\text{kprof}_{\text{TD}} \times \text{kG}_{\text{DT}} \times \text{koff}_{\text{profT}} \times (\text{koff}_{\text{profD}} + \text{kprof}_{\text{DI}})))$ | Parameter required when lumping cytosolic reactions |

Table S3. **Global parameters** (Continued)

| Parameter name | Unit | Functional form/value | Comment |
|----------------|-----------------|---|--|
| cytQ DI | s ⁻⁷ | $((\text{cytK4} \times ((\text{cytS1} \times \text{kG_DI}) + (\text{koff_bthyD} \times \text{kbthy_DI} \times \text{kon_bthyD} \times \text{Bthy_cyt}))) + (\text{cytS1} \times \text{kprof_DI} \times \text{kon_profD} \times \text{Prof_cyt} \times ((\text{cytK1} \times \text{koff_profD}) + (\text{kprof_TD} \times \text{kG_DT} \times \text{koff_profT}))))$ | Parameter required when lumping cytosolic reactions |
| cytQ ID | s ⁻⁷ | $((\text{cytK4} \times ((\text{cytS1} \times \text{kG_ID} \times \text{Pi}) + (\text{koff_bthyD} \times \text{kbthy_ID} \times \text{Pi} \times \text{kon_bthyD} \times \text{Bthy_cyt}))) + (\text{cytS1} \times \text{koff_profD} \times \text{kprof_ID} \times \text{Pi} \times ((\text{cytK1} \times \text{kon_profD} \times \text{Prof_cyt}) + (\text{kprof_DT} \times \text{kon_profT} \times \text{Prof_cyt} \times \text{kG_TD}))))$ | Parameter required when lumping cytosolic reactions |
| cytS1 | s ⁻² | $((\text{koff_bthyD} \times \text{koff_bthyD}) + (\text{koff_bthyD} \times \text{kbthy_ID} \times \text{Pi}) + (\text{koff_bthyD} \times \text{kbthy_DI}))$ | Parameter required when lumping cytosolic reactions |
| point K1 | s ⁻² | $((\text{koff_pointI} \times \text{koff_pointD}) + (\text{koff_pointI} \times \text{kpoint_ID} \times \text{Pi}) + (\text{koff_pointD} \times \text{kpoint_DI}))$ | Parameter required when lumping pointed-end reactions with G-actin |
| point K2 | s ⁻² | $((\text{kG_DT} \times \text{r_hydrolysis}) + (\text{kon_pointI} \times \text{PointedEndTotal} \times \text{r_hydrolysis}) + (\text{kG_DT} \times \text{koff_pointI}))$ | Parameter required when lumping pointed-end reactions with G-actin |
| pointQ DI | s ⁻⁵ | $((\text{kG_DI} \times \text{pointK1} \times \text{pointK2}) + (\text{koff_pointD} \times \text{kpoint_DI} \times \text{kon_pointI} \times \text{PointedEndTotal} \times \text{pointK2}))$ | Parameter required when lumping pointed-end reactions with G-actin |
| pointQ ID | s ⁻⁵ | $((\text{kG_ID} \times \text{Pi} \times \text{pointK1} \times \text{pointK2}) + (\text{koff_pointI} \times \text{kpoint_ID} \times \text{Pi} \times \text{kon_pointD} \times \text{PointedEndTotal} \times \text{pointK2}))$ | Parameter required when lumping pointed-end reactions with G-actin |

Table S4 is available online as a pdf file and contains information describing the reactants and reactions contained in the 1:1:1, 2:2:1, and 4:2:1 Virtual Cell models.

The models describing the 1:1:1, 2:2:1, and 4:2:1 Nck-N-WASp-Arp2/3 complex mechanisms are available online as XML files.